Study the Parameters Affect on Pump Intake Design Using CFD.

Gamal Helmy Elsayed[1], Mohamed Fayek Abd Rabbo[2], Mostafa Abuzeid[3], Elzahry Farouk Elzahry[4], and Ashraf Ghanem[5].

1.Professor of Hydraulic Dept., Faculty of Engineering at Shoubra, Benha University, Egypt.
2.Professor of Mechanical Dept., Faculty of Engineering at Shoubra, Benha University, Egypt.
3.Director of Mechanical and Electrical Research Institute at MWRI.
4.Associate Professor of Hydraulic Dept., Faculty of Engineering at Shoubra, Benha University, Egypt.
5.Ph. D Student, Faculty of Engineering at Shoubra, Benha University, Egypt.

*Corresponding author: (ashraf_ghanem@outlook.com).

Abstract: The basic purpose of a pump intake is to supply water with a uniform velocity at the entry of an impeller. The fluid flow in Pump intakes is rather complex involving expansions and turns together with fluid-structure interactions. The intake of pumps is usually designed analytically, based on standard designs, best practices and also previous implementation experience. These basic designs are often updated to accommodate varying pump flow rates or different site limitations. Such changes can affect approach flow characteristics and result in underperformance of pumps. Pumps are known to experience common operational problems such as decreased flow rate and head, power effects, and increased vibration and noise. Pumps can in extreme cases experience impeller corrosion due to cavitation and excessive wear of shafts, bearings, wear rings, and couplings. This results in a Lack of pump efficiency and reliability degradation, which leads to a significant increase in operating and maintenance costs. Such issues are related to certain undesirable characteristics of the approach flow and are caused primarily by poor design of the pump intake structure. Due to the high cost of the construction and operation of laboratory models and the limited measurements taken, the utilization of numerical modeling as an alternative tool for studying complex flow problems has become popular with the rapid development of Computational Fluid Dynamics (CFD) software. we can predict the flow parameters at the pump inlet with the change in geometry without actual running of the pump with CFD. Hence the design of the sump can be optimized to keep the flow parameters below limiting values. This study attempts to Study the Parameters Affect on Pump Intake Design and model the flow characteristic in a pump sump, minimize the swirl angles, increase the flow at the pump inlet and keep the flow parameters below limiting values. by using (CFD) code FLUENT. The numerical study carried out in this paper aims at optimizing the overall fluid flow in a pump intake by the use of a commercially available CFD code. CFD study was carried out on initial sump geometry and initial CFD results were analyzed.

Keywords: CFD, Pump Intake, Vortexes, pumping station.

1. INTRODUCTION

Desmukh and Gahlot [1] studied the flow conditions at the entry to a pump depend Upon flow conditions in the location of pump intake concerning the walls, sump geometry, approach channel, velocity changes, and obstructions such as piers, screens, etc. , and rotational tendencies inflow produced upstream of the pump bays In his work, he has attempted to simulate and predict the flow conditions such as swirl and vortices for multiple pump intakes in a single sump to determine the viability of, commercially available computational fluid dynamic software – ANSYS CFX as an important design optimization tool for intake sumps. And they concluded that the commercial CFD package ANSYS CFX-10 was used to predict the three-dimensional flow and vortices in a pump sump model. Ashraf Ghanem and Elzahry Farouk Elzahry [2] studied the hydraulic problems in the Faraskour pumping station. Initially, water could not reach the first and fifth units of the operation. The main hydraulic problem of the suction basin of the new pump station is the sharp rotation of the suction guide from the sharp rotation of the quay station, and that caused the continuous discontinuation of the first and fifth units due to the lack of regular water entering the unit. A numerical simulation was conducted to investigate the hydraulic stability of the station. Computational fluid dynamic (CFD) is used to simulate the flow conditions at different working pumping units to predict the hydraulic problem at the suction side. The results indicate that the geometry of the intake is proper for running five parallel flow pumps with the designed flow rate and use guide walls with a curvature length of 6 m and width of 0.5 m for each pump. Cecilia et al [3] aimed at verifying the ability of a commercial computational fluid dynamic (CFD) code to predict the formation of vortices in a pump sump. The intention was to identify intensity in a geometrically simple pump sump and vortices of diverse origin of which experimental results under the same operating conditions are known. Calculated velocities correlate well to Magnitudes and trends of measured ones, whereas the maximum values of vortices calculated are several orders of magnitude higher than those measured, which is explained by the characteristics of measurement in the physical model. They concluded that the

results allow establishing some conclusions regarding the application of the FLOW-3D code for detecting vortices in a pump sump using the LES (Large Eddy Simulation) model. The latter has been suggested in the references instead of other turbulence models like the Reynolds Averaged Navier-Stokes (RANS) which does not represent realistically the highly unstable and intermittent phenomenon. The numerical results demonstrated the capability of the model identifying the observed vortices in the physical model. Franci et al [4] make computational fluid dynamics (CFD) calculation of pump sumps which troublesome due to the nature of the flow. Pump sump flow is unsteady and turbulent, and pump sump dimensions were large compared to the diameter of vortices occurring near the sump walls or in the pump column. Therefore, the computational grid should be fine enough in certain areas of the sump, to capture the general and important phenomena of the flow. An important role played by the decision for the suitable turbulent model, in adding or reducing the computational costs. The present work intends to get an answer whether the Unsteady Reynolds Averaged Navier-Stokes (URANS) model fails in predictions of vortex modeling since the usage of the Large Eddy Simulation (LES) model for industrial cases would represent huge computational power demands. In the second part of the paper, a real case pump sump is analyzed. Elzahry Farouk Elzahry and Ashraf Ghanem [5] studied the hydraulic problem in A New El-Tabiya pumping station in Alexandria Governorate. The station consists of six axial pumping units. The numerical study carried out in this paper aims at optimizing the overall fluid flow in a pump intake by the use of a commercially available CFD code. CFD study was carried out on initial sump geometry and initial CFD results were analyzed. The study of vortex formation in pump sump during intake for pumps with wet pit installation has been an ongoing effort by many researchers for the past decades. Although vortices may occur in dry pit installation as well, the effects are more detrimental for the wet pit installation due to the fact that the pump inlet is submerged in water and therefore the vortices can directly come in contact with the pump impeller and cause damages which will affect the pump performance [6]. This work will complement vortex-reduction effort in intake pipe which eventually affect impeller and pump performance [7]. There are guidelines proposed by organizations related to pump intake design such as ANSI [8], BSI [9] and JSME [10] which could help eliminate or at least control the formation of vortices in pump sump. These guidelines mainly focus on the geometry of the pump sump in the vicinity of the inlet where sharp edges or curvatures in the sump may alter the uniformity of the intake flow and thus create high vorticity regions which will be the source of vortex formation [11].

2. Problem Statement

Pump intakes are hydraulic structures used to withdraw water from a river or reservoir; poor intake design can result in submerged or surface vortices, flow swirls entering the pump, non-uniform velocity distribution at the pump impeller, and air or gas bubbles being drawn in. The flow at the impeller must restrict the degree to which these hydraulic conditions are present for pumps to achieve their maximum hydraulic efficiency in all operating conditions. Therefore, testing the pump intakes using an experimental model or a numerical model was necessary to predict the flow characteristics accurately. Due to the high cost of the construction and operation of laboratory models and the limited measurements taken, the utilization of numerical modeling as an alternative tool for studying complex flow problems has become popular with the rapid development of Computational Fluid Dynamics (CFD) software and studying the Parameters Affect on Pump Intake Design Using CFD such as discharge in the canal and water level.

3. Simulation Procedure

Before the simulation can be made, many constraint factors have to be considered. The computer model setup is generated by the pre-processor. Then the type of meshing has been selected before the problem is solved. The boundary conditions have to be carefully set up because most of the input parameters are based on the boundary conditions. After the mesh generation is completed, the problem will be solved by a solver. In solver, the quality of the mesh will be evaluated. If mesh quality is poor, then it has to be refining until it was successfully read by the solver. The solver formulation, turbulence model which compensates the fluctuating velocity terms and material properties, has to be decided for calculating the flow field of the body. After the boundary condition and the solution control parameter is specified, the problem is ready to be initialized. The initializing and iteration processes will stop when the calculations are accomplished. Then the results can be examined and analyzed. For the present study.

4. Numerical Model

The numerical model for the case study is then built using ANSYS fluent 18.1 and the geometry is drawn using the design modeler, a suitable set up of the solution of the numerical model is set and the numerical results are extracted and compared to the recommendations of the standard ANSI 9.81/2012. To get an accurate simulation, the outlet volume flow is applied in these cases. The numerical analysis is a transient state. The “ideal wall” condition simulates the level of water, while the environment pressure condition is applied to simulate on the “inlet caps”. The quality of the computational mesh has an important role in achieving the desired accuracy of the simulations especially if the computational domain is very complex. The basic three-dimensional geometry is prepared using The ANSYS R18.1 software. The equations are supplemented by

fluid state equations defining the nature of the fluid, and by empirical dependencies of fluid density, viscosity, and thermal conductivity on temperature. To predict turbulent flows, the Favre-averaged Navier-Stokes equations are used, where time-averaged effects of the flow turbulence on the flow parameters are considered, where the other, i.e. large-scale, time-dependent phenomena are taken into account directly. Three-dimensional unstructured meshes are used for the flow simulation in the pump sump. The unstructured mesh is used for this study due to model complexity and easy to mesh especially at the intake section. The numerical solver uses unstructured meshes that allow flexibility in meshing very complex geometries while maintaining high-quality computational mesh which is necessary for obtaining accurate solutions. The solver requires some initial values for initializing the finite element analysis procedure. These initial values approximate the required conditions. The inlet boundary condition is applied at the entry in terms of total mass flow that is entering into the sump, using a high-intensity turbulence model. This model is chosen to keep the frictional, turbulence errors in consideration. At the outlet face, an outflow is assumed averaging over the entire face. There is no slip in the wall and the surfaces of the sump are kept smooth to reduce friction losses as much as possible.

4. MESH DESCRIPTION

The meshing technique used is the tetrahedrons method with inflation to all solid walls of the channel and suction pipe. Furthermore, to enhance the solution accuracy and solution speed the tetrahedrons mesh was being converted to polyhedrons mesh as shown in figures (1) and (2). the number of mesh elements and computational nodes are within the range of 2928869 and 1063169 respectively.

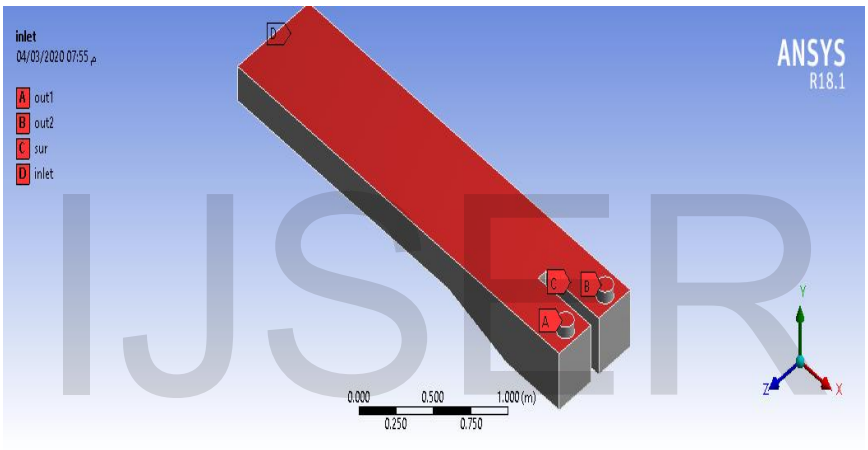

Fig. (1) The boundary conditions setup.

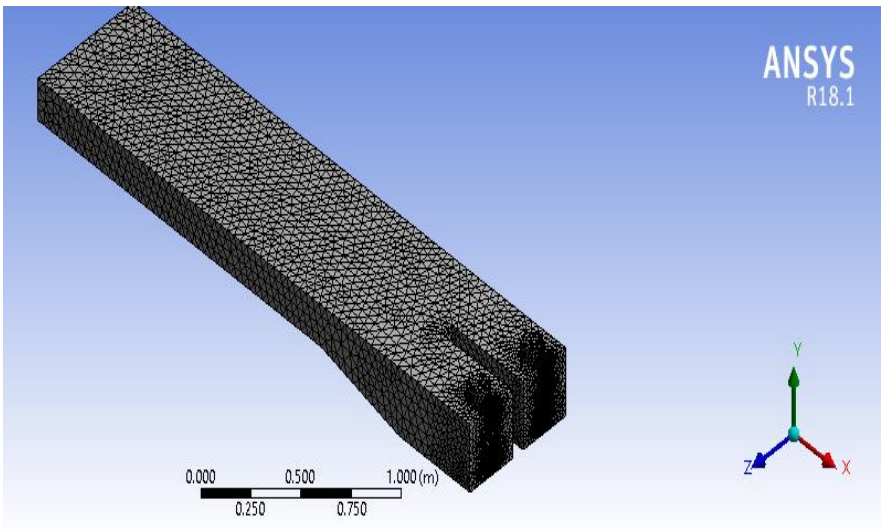

Fig. (2) Mesh distributed across a 3D view.

5. SOLUTION SETUP

The boundary conditions of the solution technique are indicated on a 3D model in figure 1. the turbulence model used in the solution technique is RNG- K -ε model. This model was selected due to its good agreement between the numerical solution and the experimental work. the quality of the computational mesh has an important role in achieving the desired accuracy of

the simulations especially if the computational domain is very complex. The basic three-dimensional geometry is prepared using The ANSYS R18.1 software flow simulation software drawing with the grid surfaces plot of a sump. The equations are supplemented by fluid state equations defining the nature of the fluid, and by empirical dependencies of fluid density, viscosity, and thermal conductivity on temperature. To predict turbulent flows, the Favre-averaged Navier-Stokes equations are used, where time-averaged effects of the flow turbulence on the flow parameters are considered, where the other, i.e. large-scale, time-dependent phenomena are considered directly. Three-dimensional unstructured meshes are used for the flow simulation in the pump sump. The unstructured mesh is used for this study due to model complexity and easy to mesh especially at the intake section. The numerical solver uses unstructured meshes that allow flexibility in meshing very complex geometries while maintaining high-quality computational mesh which is necessary for obtaining accurate solutions.

6. SWIRL ANGEL

One of the most important parameters that is also used to determine whether the pump intake is acceptable or not is the swirl angel. Where the acceptance criteria for swirl angel as discussed previously is 5° [12].

$$\theta = \tan^{-1} \frac{V_t}{V_A}$$

Where,

V_t = Tangential velocity in suction pipe (m/s)

V_A = Axial velocity in suction pipe (m/s)

7 .RESULTS AND DISCUSSIONS

7.1. EFFECT OF DISCHARGE:

The canal capacity always changes throughout the year and the most important reason for this change is the winter intensity in January and the climate changes affecting the efficiency of pumps, Figures (1) through (9), developed directly from FLUENT under ANSYS 18.1 software output, illustrate the results of cases 1,2 and 3 of the model simulation which represents the effect of the discharge. In each of these figures, the magnitudes of velocity vectors (in m/s), streamline shape and its directions and velocity contour are indicated by the color scale and the length of each vector depends on the direction of the velocity. The velocity vector (m/s) contours had been shown in this section. These figures were included to illustrate the basic features of model output.

	Water Level (m)	Discharge (L/Sec)
Case 1	0.3	30
Case 2	0.3	15
Case 3	0.3	10

7.1.1. VELOCITY VECTOR AT THE WATER LEVEL OF 0.3M WITH A FLOW RATE OF 30L/S (CASE 1)

Figure (1) show the plan views of intake at the surface (0.3m), 0.15m, and bottom (0m), respectively. This case was operated at a water level of 0.3m which is the surface of the contact with the air with a flow rate of 30L/s. The velocity vectors in Fig. (1) illustrated surface vortex at the upper level of the water (at an elevation of 0.3m). There are no separation zones and the dead zone disappears and there is regularity in the streamlines as well as the vortices clearly and there is no vortex.

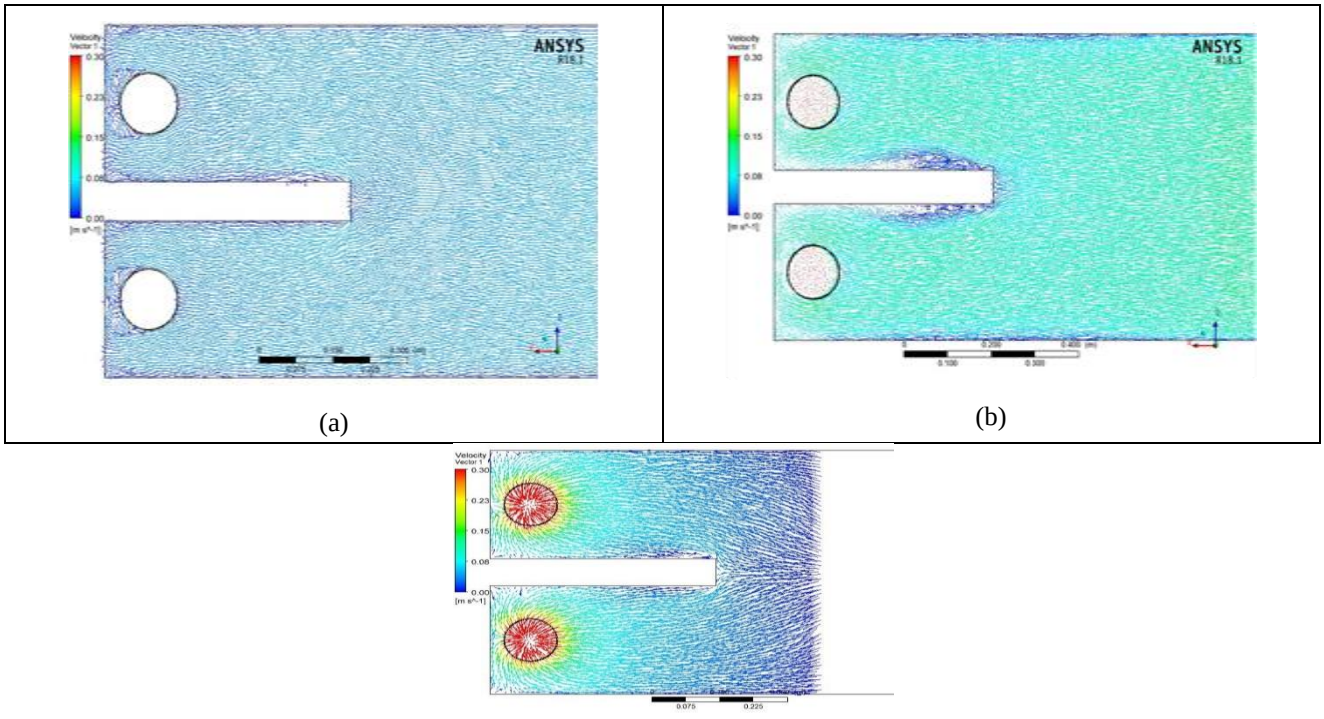

(a) (b)

(c)

Fig. (1) velocity vectors with a flow rate of 30L/s (a) at the upper level of the water (0.3m) (b) at 0.15 m (c) at the bottom(0m).

Figure (2a) illustrates the contour of velocity magnitude along the pump axis. The result shows that the velocity distribution increase and no dead zone. Figure (2b) shows the velocity vectors along the pump axis indicate that the flow is regularity and dense, and there is no dead zone.

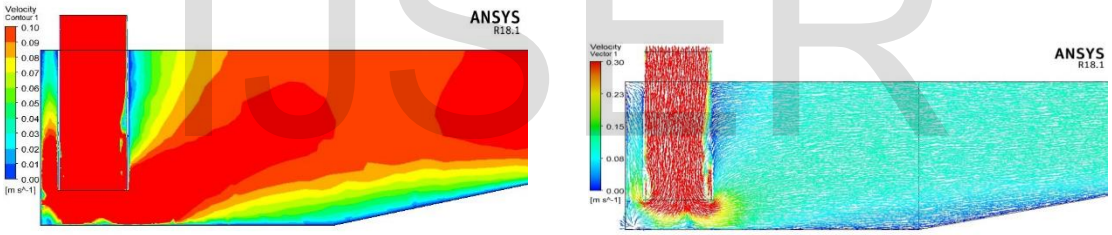

(a) (b)

Fig. (2) (a)Velocity contour (b) velocity vectors with a flow rate of 30L/s along the pump axis at water level 0.3m.

Figure (3) shows the Velocity contour, streamline velocity, and velocity vectors at the slop of the canal for case 1. The result shows that the velocity distribution increase and no dead zone and clear in the velocity vectors that the flow is regularity and dense, and there is no dead zone, and the streamline is a regularity.

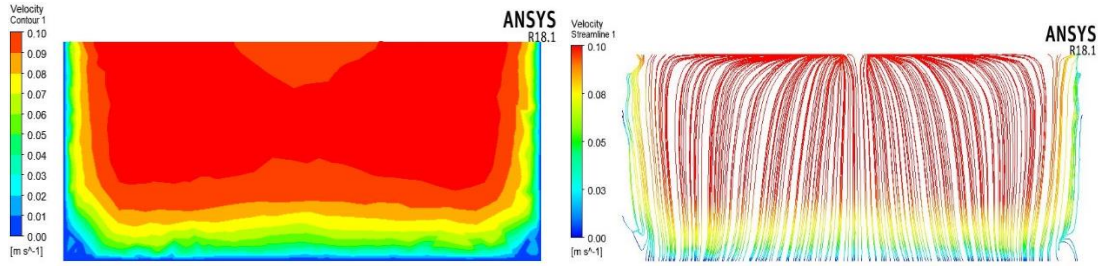

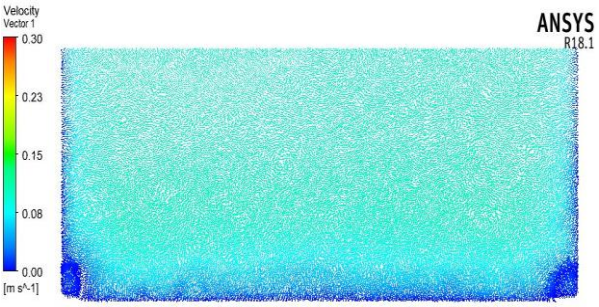

fig. (3) velocity contour, streamline velocity, and velocity vectors at the slop of canal for case 1.

7.1.2. Velocity vector at the water level of 0.3m with a flow rate of 15L/s (case 2)

This section revealed the results of the velocity vector at water level 0.3m with a flow rate of 15L/s. This case was operated at a water level of 0.3m which is the surface of the contact with the air with a flow rate of 15L/s. The velocity vectors in Fig. (4) illustrated surface vortex at the upper level of the water (at an elevation of 0.3m). A closer review of this figure reveals that there is no vortex appeared at the back of the pump column but the separation zone appeared. The location of the separation zone of the flow is symmetrically located at the back of the intake pipe 1 and 2 respectively. The effect of the low capacity of water leads to irregularity in the streamlines and the dead zone began to appear.

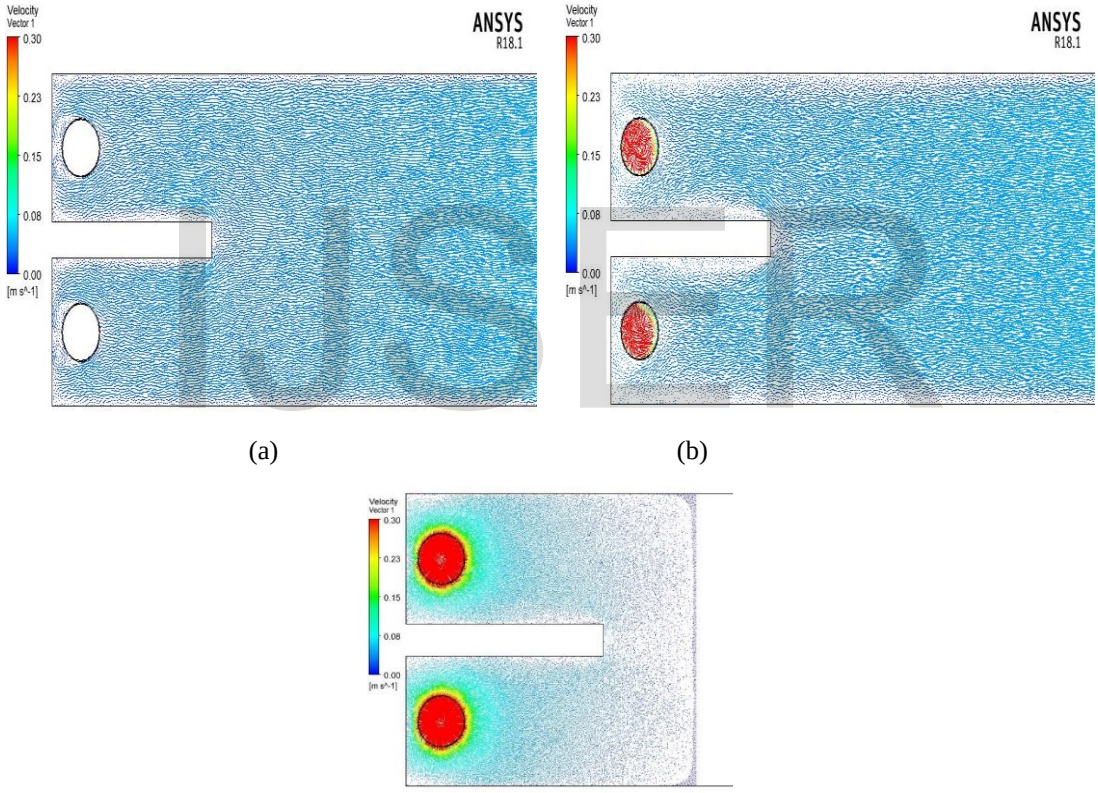

Fig. (4) velocity vectors with a flow rate of 15L/s (a) at the upper level of the water (0.3m) (b) at 0.15 m (c) at the bottom(0m).

Figure (5a) illustrates the contour of velocity magnitude along the pump axis. The result shows that the velocity distribution decrease and the dead zone appeared compared to the previous case. Figure (5b) shows the velocity vectors along the pump axis indicate that the flow is an irregularity, and there is a separation zone compared to the previous case.

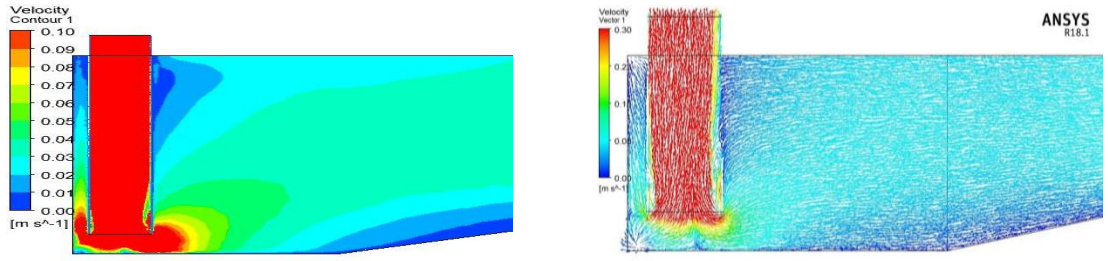

(a) (b)

Fig. (5) (a)Velocity contour (b) velocity vector with a flow rate of 15L/s along the pump axis.

Figure (6) shows the Velocity contour, streamline velocity, and velocity vectors at the slop of the canal for case 2. The result shows that the velocity distribution decrease and the dead zone appear and clear in the velocity vectors that the flow is an irregularity and there is a separation zone, and the streamline is irregularity and divergence towards the sidewall compared to the previous case.

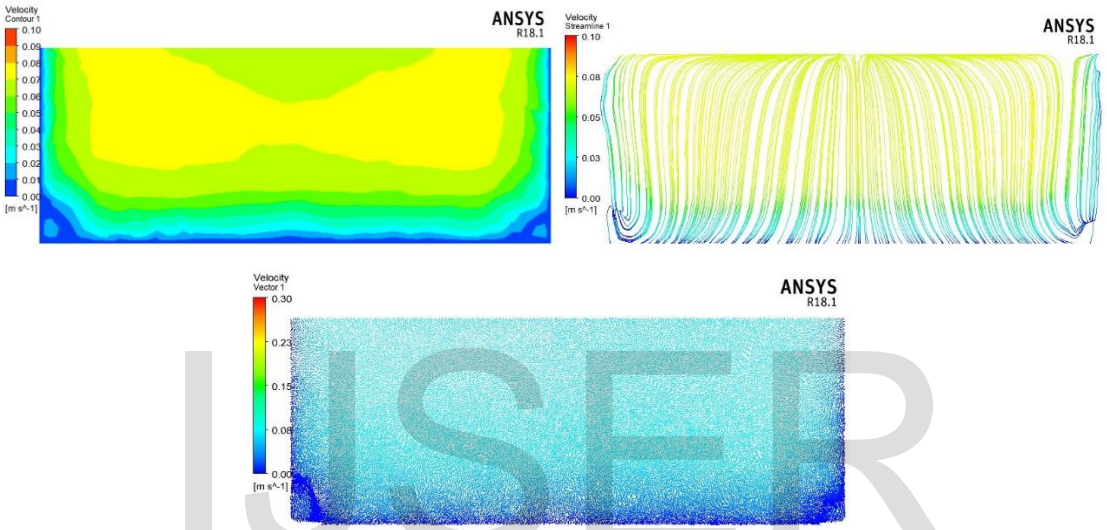

Fig. (6) Velocity contour, streamline velocity, and velocity vectors at the slop of canal for case 2.

7.1.3. VELOCITY VECTOR AT THE WATER LEVEL OF 0.3M WITH A FLOW RATE OF 10L/S (CASE 3)

This section revealed the results of the velocity vector at water level 0.3m with a flow rate of 10L/s. This case was operated at a water level of 0.3m which is the surface of the contact with the air with a flow rate of 10L/s. The velocity vectors in Fig. (7) illustrated surface vortex at the upper level of the water (at an elevation of 0.3m). this figure reveals that the separation zone appeared and increase at the around of the pump column. The location of the separation zone of the flow is symmetrically located at the back of the intake pipe 1 and 2 respectively. The effect of the low capacity of water leads to irregularity in the streamlines and the dead zone began to appear.

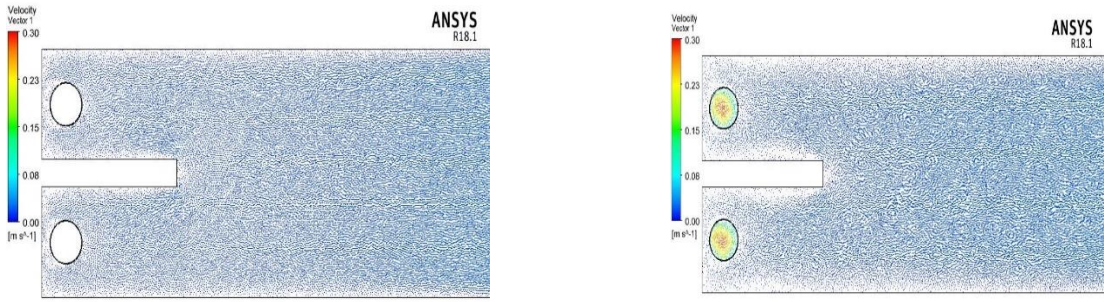

(a) (b)

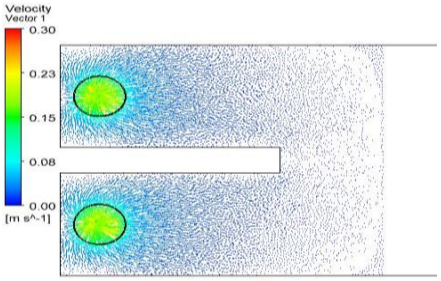

(c)

Fig. (7) velocity vectors with a flow rate of 10L/s (a) at the upper level of the water (0.3m) (b) at 0.15 m (c) at the bottom (0 m).

Figure (8a) illustrates the contour of velocity magnitude along the pump axis. The result shows that the dead zone increase around the suction pipe and the velocity of the flow decrease compared to the previous case. Figure (8b) shows the velocity vectors along the pump axis indicate that the flow is an irregularity, and there is a separation zone compared to the previous case.

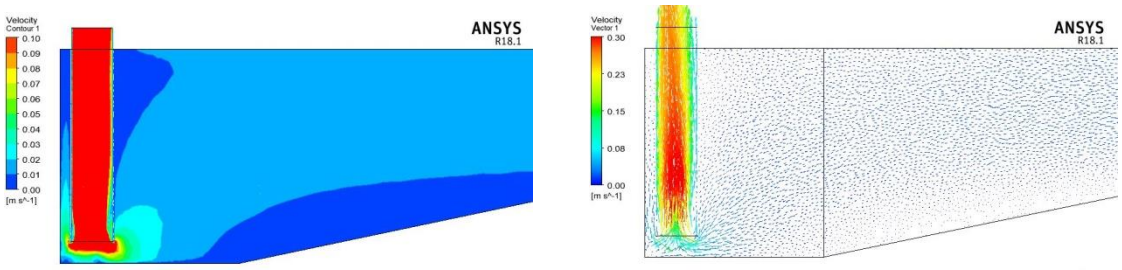

(a) (b)

Fig. (8) (a)Velocity contour (b) velocity vector with a flow rate of 4L/s along the pump axis.

Figure (9) shows the Velocity contour, streamline velocity, and velocity vectors at the slop of the canal for case 3. The result shows that the velocity distribution decrease and the dead zone appear and clear in the velocity vectors that the flow is an irregularity and there is a separation zone, and the streamline is irregularity and divergence towards the sidewall compared to the previous case.

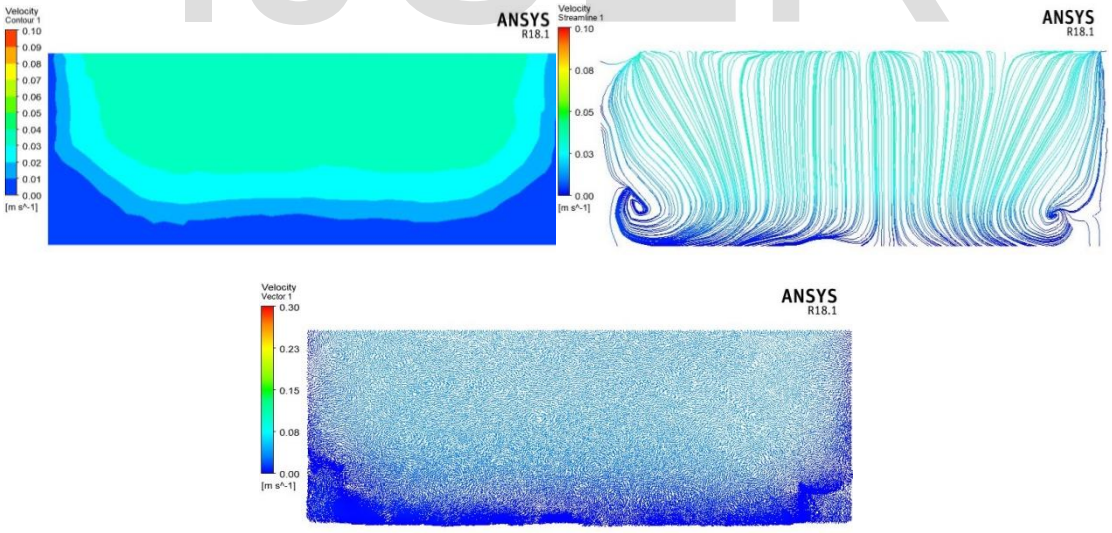

Fig. (9) Velocity contour, streamline velocity, and velocity vectors at the slop of canal for case 3.

From the above results the increasing discharge in the canal leads to increase water velocity and there is no dead zone in the sump pump in the same section when the water level is constant.

7.2. Effect of Water Level in the Canal:

The water level is low due to depositions that occur at the pump intake, Figures (10) through (19), developed directly from FLUENT under ANSYS 18.1 software output, illustrate the results of cases 4,5 and 6 of the model simulation which represents the effect of the deposition in the canal. In each of these figures, the magnitudes of velocity vectors (in m/s), streamline shape and its directions and velocity contour are indicated by the color scale and the length of each vector depends on the direction

of the velocity. The velocity vector (m/s) contours had been shown in this section. These figures were included to illustrate the basic features of model output.

	Water Level (m)	Discharge (L/Sec)
Case 4	0.18	30
Case 5	0.12	30
Case 6	0.06	30

7.2.1. VELOCITY VECTOR AT THE WATER LEVEL OF 0.18M WITH A FLOW RATE OF 30L/S (CASE 4)

Figure (10) show the plan views of intake at the surface (0.18m), 0.09m, and bottom (0m), respectively. This case was operated at a water level of 0.182m which is the surface of the contact with the air with a flow rate of 30L/s. The velocity vectors in Fig. (10) illustrated surface vortex at the upper level of the water (at an elevation of 0.18m). There are no separation zones and the dead zone disappears and there is regularity in the streamlines as well as the vortices clearly and there is no vortex.

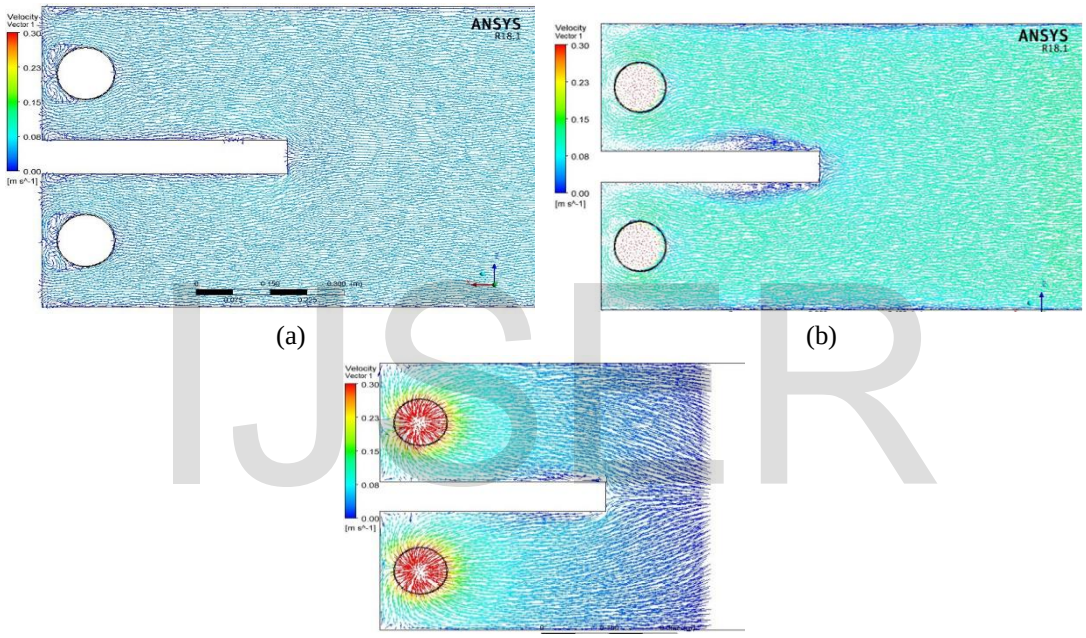

(a) (b)

(c)

Fig. (10) velocity vectors with a flow rate of 30L/s (a) at the upper level of the water (0.182m) (b) at 0.09 m (c) at the bottom(0m).

Figure (11a) illustrates the contour of velocity magnitude along the pump axis. The result shows that the velocity distribution increase and the no dead zone. Figure (11b) shows the velocity vectors along the pump axis indicate that the flow is regularity and dense, and there is no dead zone.

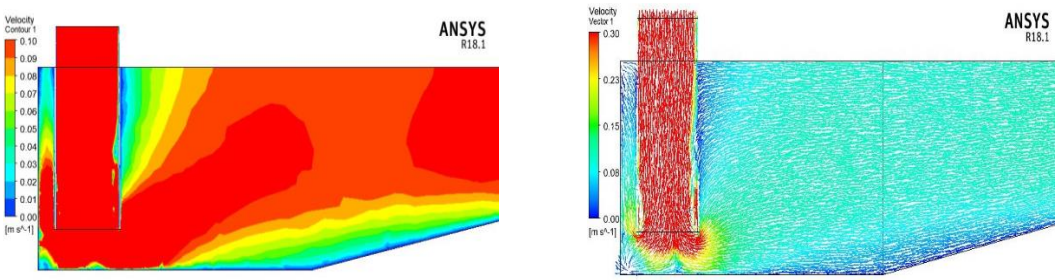

(a) (b)

Fig. (11) (a)Velocity contour (b) velocity vectors with a flow rate of 30L/s along the pump axis at water level 0.18m.

Figure (12) shows the Velocity contour, streamline velocity, and velocity vectors at the slop of the canal for case 4. The result shows that the velocity distribution increase and the no dead zone and clear in the velocity vectors that the flow is regularity and dense, and there is no dead zone and the streamline is a regularity.

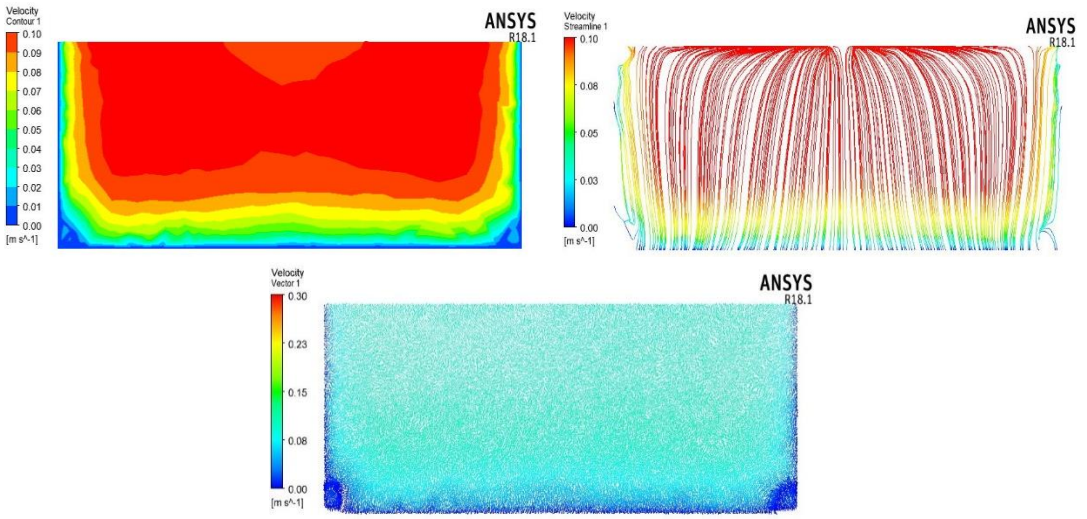

Fig. (12) Velocity contour, streamline velocity, and velocity vectors at the slop of canal for case 1.

7.2. 2. VELOCITY VECTOR AT THE WATER LEVEL OF 0.12M WITH A FLOW RATE OF 30L/S (CASE 5)

This section revealed the results of the velocity vector at water level 0.12m with a flow rate of 30L/s. This case was operated at a water level of 0.12m which is the surface of the contact with the air with a flow rate of 30L/s. The velocity vectors in Fig. (13) illustrated surface vortex at the upper level of the water (at an elevation of 0.12m). A closer review of this figure reveals that one counter-rotating vortex appeared at the back of the pump column. The location of the vortex is symmetrically located at the back of the intake pipe 1 and 2 respectively and there are separate zones of the flow. The occurrence of the surface vortex also appeared at similar locations, which shows the velocity vector at the elevation of 0.06m. As expected, the vortices at this elevation (0.06m) of the pump sump intake are slightly smaller than those shown at the surface The effect of the low water level leads to irregularity in the streamlines, and the dead zone began to appear as well as the vortices clearly compared to previous cases.

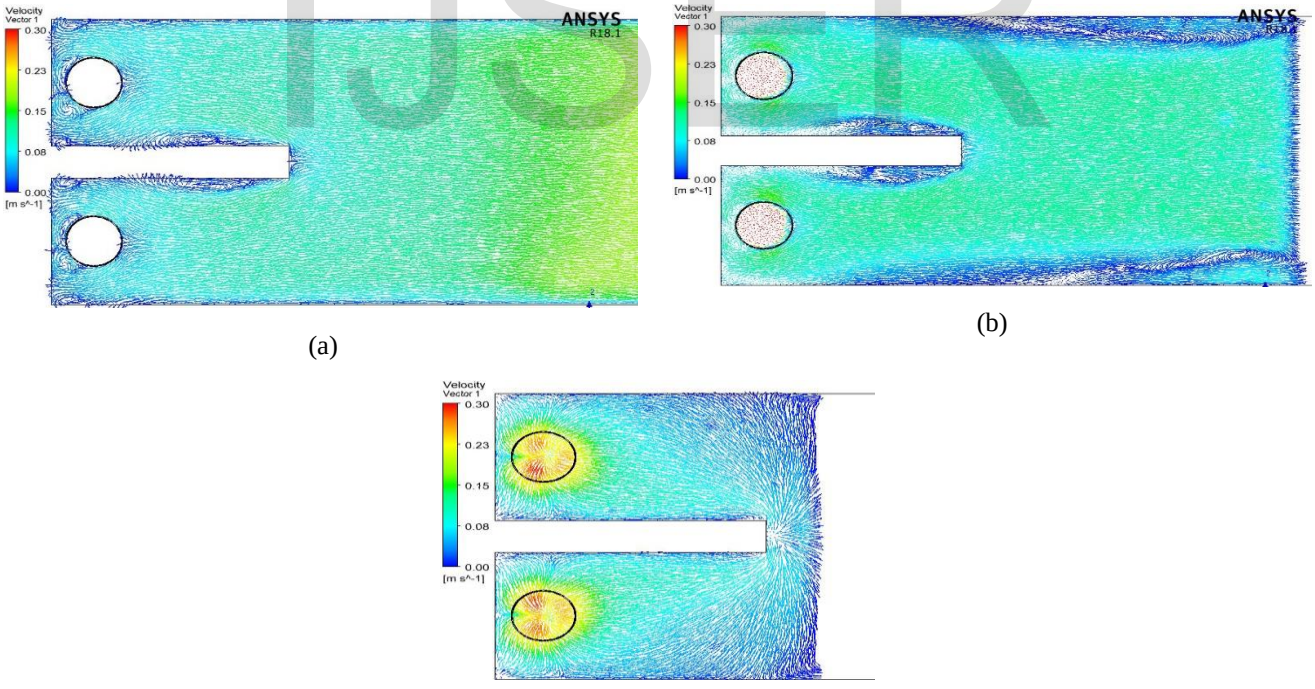

Fig. (13) velocity vectors with a flow rate of 30L/s (a) at the upper level of the water (0.12m) (b) at 0.06 m (c) at the bottom(0m).

Figure (14a) illustrates the contour of velocity magnitude along the pump axis. The result shows that the velocity distribution decrease and the dead zone appeared compared to the previous case. Figure (14b) shows the velocity vectors along the pump axis indicate that the flow is an irregularity, and there is a separation zone compared to the previous case.

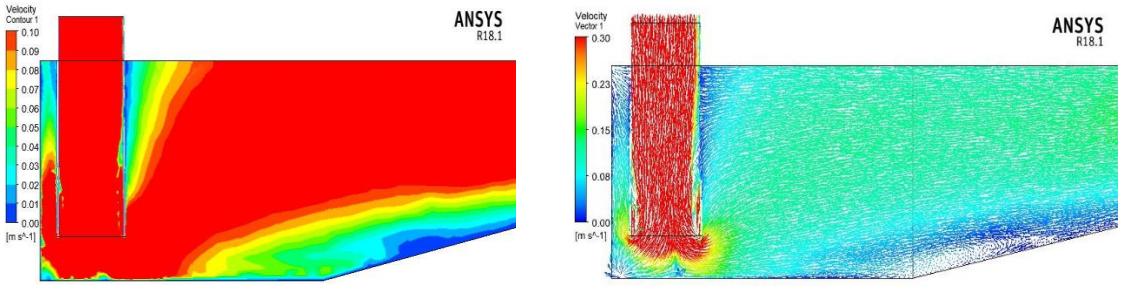

(a) (b)

Fig. (14) (a)Velocity contour (b) velocity vectors with a flow rate of 30L/s along the pump axis at water level 0.12m.

Figure (15) shows the Velocity contour, streamline velocity, and velocity vectors at the slop of the canal for case 5. The result shows that the velocity distribution decrease and the dead zone appear and clear in the velocity vectors that the flow is an irregularity and there is a separation zone, and the streamline is irregularity and divergence towards the sidewall compared to the previous case.

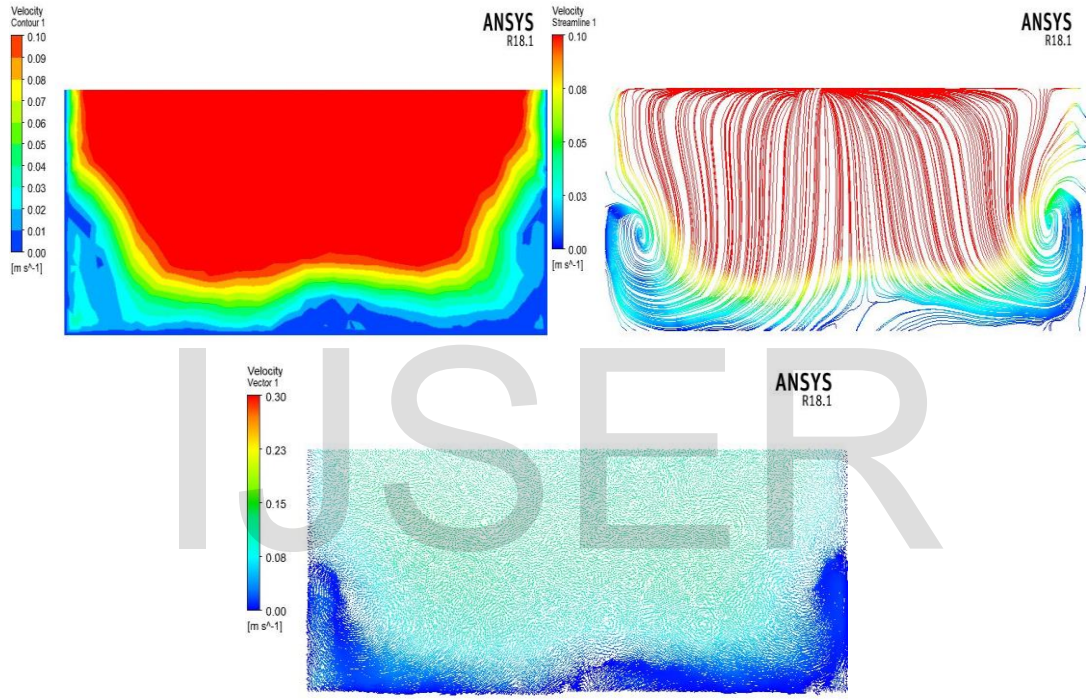

Fig. (15) Velocity contour, streamline velocity, and velocity vectors at the slop of canal for case 5.

7.2. 3. VELOCITY VECTOR AT THE WATER LEVEL OF 0.06M WITH A FLOW RATE OF 30L/S (CASE 6).

Figure (16) illustrates the contour, vector, and streamline of velocity magnitude at the upper level of the water (0.06m). There are separation zones and the dead zone appears and there is an irregularity in velocity vectors as well as the vortices clearly compared to previous cases. One rotating surface vortex type 4 to 5 behind the column intake, one subsurface vortex type2 directly under the intake column, and one wall attach vortex respectively at the back and side wall (inner and outer).

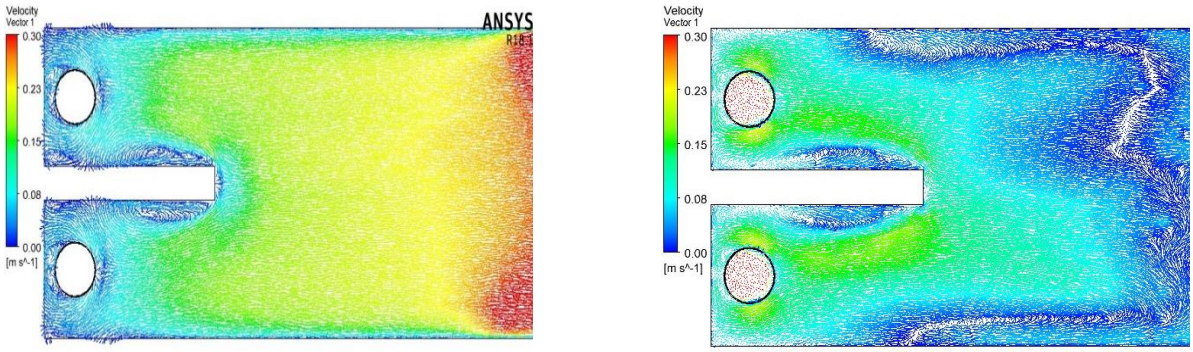

(a) (b)

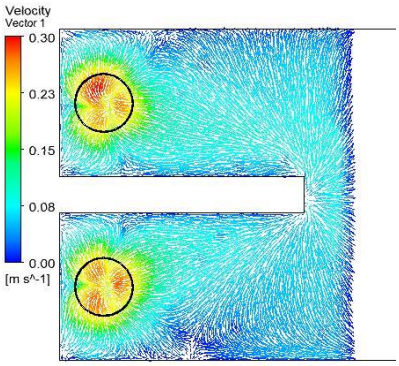

(c)

Fig. (16) velocity vectors with a flow rate of 30L/s (a) at the upper level of the water (0.06m) (b) at 0.03 m (c) at the bottom (0 m).

Figure (17a) illustrates the contour of velocity magnitude along the pump axis. The result shows that the velocity distribution decrease and the appearance of the dead zone clearly in the slop of the canal compared to the previous case. Figure (17b) shows the velocity vectors along the pump axis indicate that the flow is an irregularity, an and Increase in the appearance of the separation zone behind the column of the suction pipe compared to the previous case.

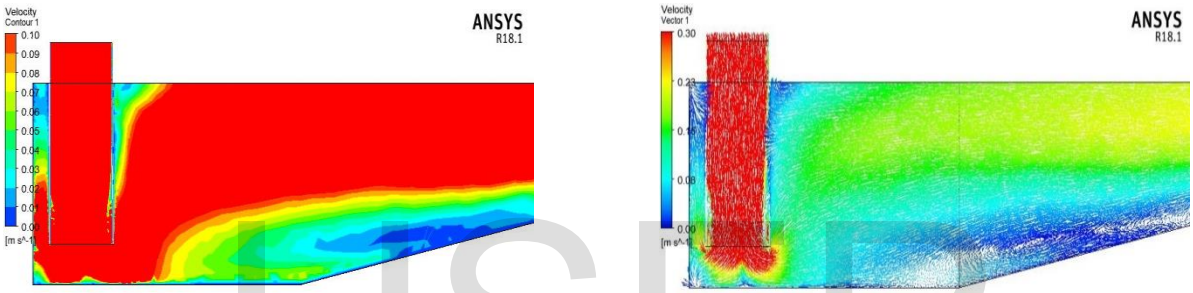

(a) (b)

Fig. (17) (a)Velocity contour (b) velocity vectors with a flow rate of 30L/s along the pump axis at water level 0.06m.

Figure (18) shows the Velocity contour, streamline velocity, and velocity vectors at the slop of the canal for case 6. The result shows that the velocity distribution decrease and the dead zone appear and clear in the velocity vectors that the flow is an irregularity and there is a separation zone, and the streamline is irregularity and divergence towards the sidewall compared to the previous case.

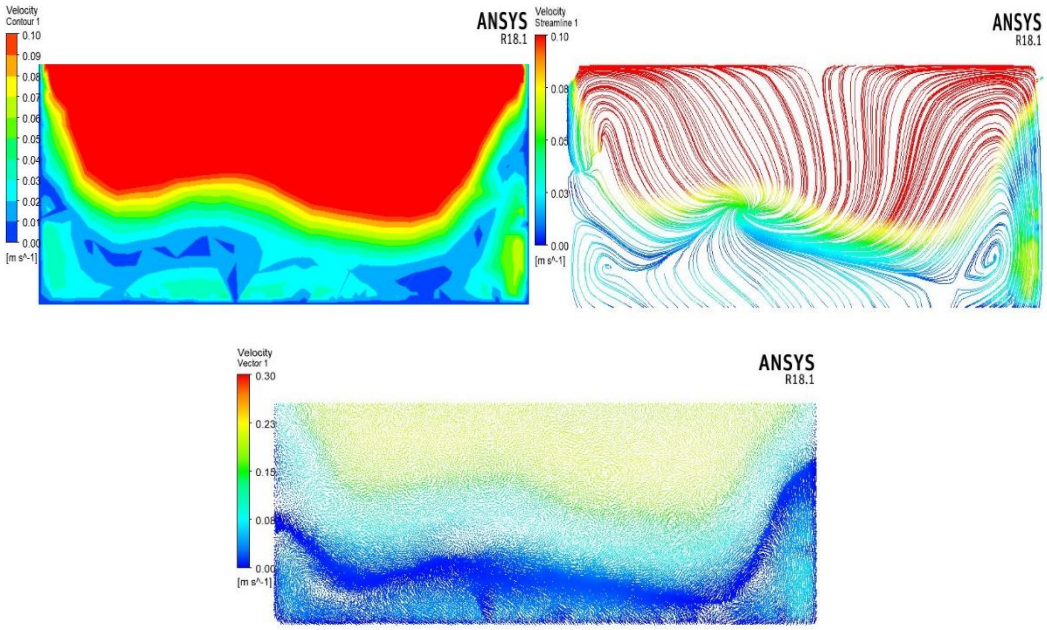

Fig. (18) Velocity contour, streamline velocity, and velocity vectors at the slop of canal for case 21.

From above results The increasing water level in the pump sump leads to increase water velocity and there is no dead zone in the same section when discharge is constant.

7.3. EFFECT HEIGHT OF PUMP SUMP:

Three cases are studied to know the effect of sump height on the flow of water, Figures (19) through (24), illustrate the results of cases 7, 8 and 9 of the model simulation which represents the effect of the height. In each of these figures, the magnitudes of velocity vectors (in m/s), streamline shape and its directions and velocity contour are indicated by the color scale and the length of each vector depends on the direction of the velocity. The velocity vector (m/s) contours had been shown in this section. These figures were included to illustrate the basic features of model output.

	Length (m)	Discharge (L/Sec)
Case 7	0.3	30
Case 8	0.24	30
Case 9	0.18	30

Figure (19) shows the velocity vectors along the pump axis indicate that the flow is an irregularity, and there is a separation zone when the height increases, in case no 7 the slop had a bad effect on the flow, velocity decreases and there is a dead zone.

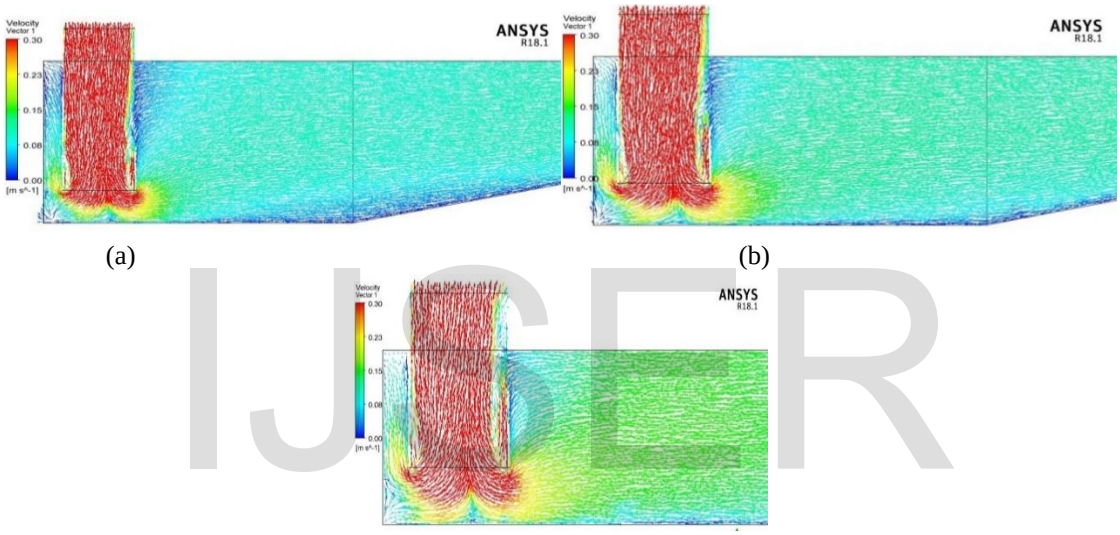

(a) (b)

(c)

Fig. (19) velocity vectors along the pump axis (a) case 7 (b) case8 (c) case9.

Figure (20) shows the velocity contour along the pump axis indicates that the velocity of flow increases when the height of the sump decreases, and there is no separation zone, in case no 1 the slop had a pad effect on the velocity of flow.

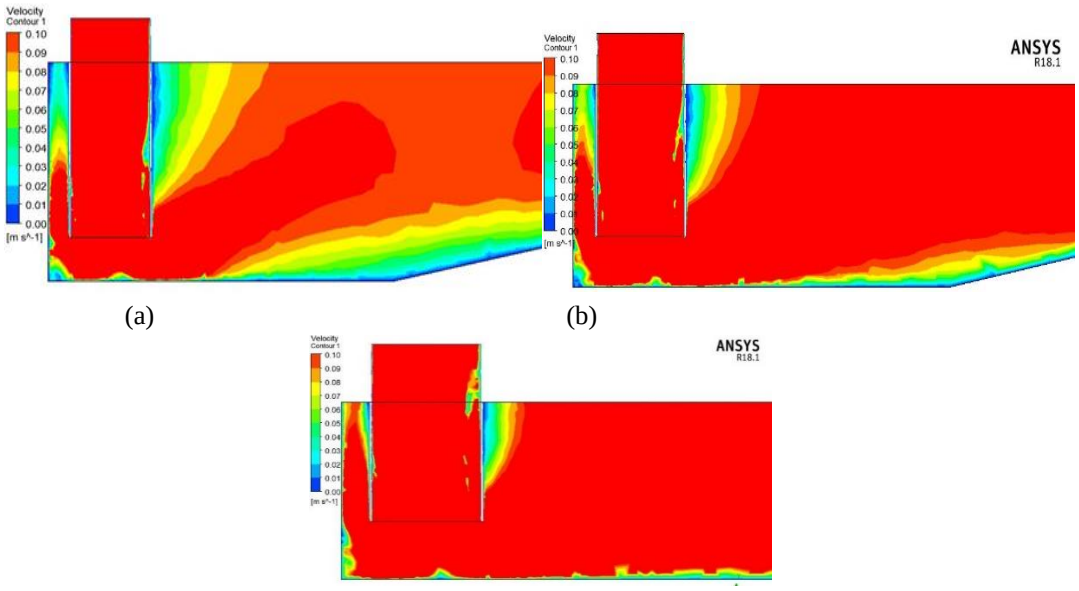

(a) (b)

(c)

Fig. (21) velocity contour along the pump axis (a) case 7 (b) case8 (c) case9.

Figure (22) shows the velocity vectors along the suction pipe indicate that the flow is an irregularity, and there is a separation zone when the height increases, in case no 7 the slop had pad effect on the flow, velocity decreases and there is a dead zone.

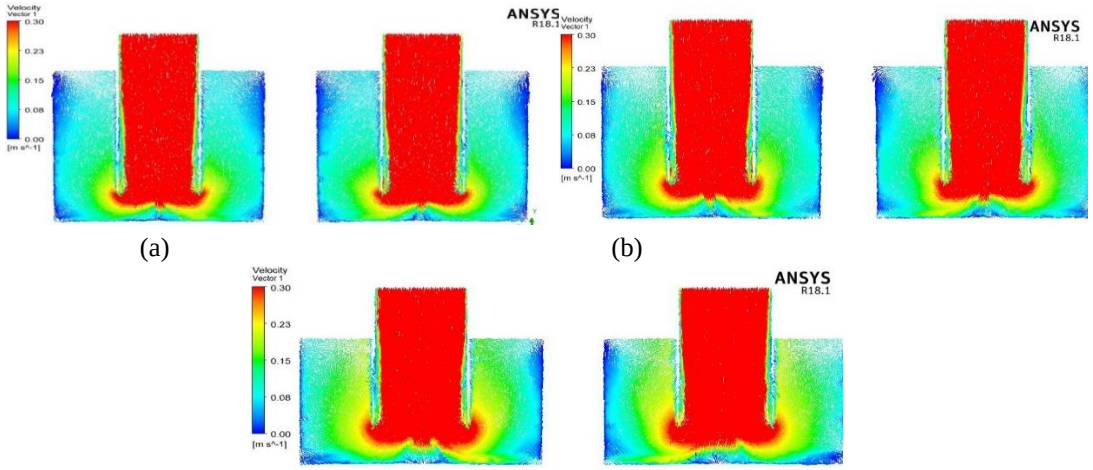

(a) (b)

(c)

Fig. (22) velocity vectors along the suction pipe (a) case 7 (b) case8 (c) case9.

The velocity contour along the pump axis shown in Figure (23) indicates that the velocity of flow increases when the height of the sump decreases, and there is no dead zone.

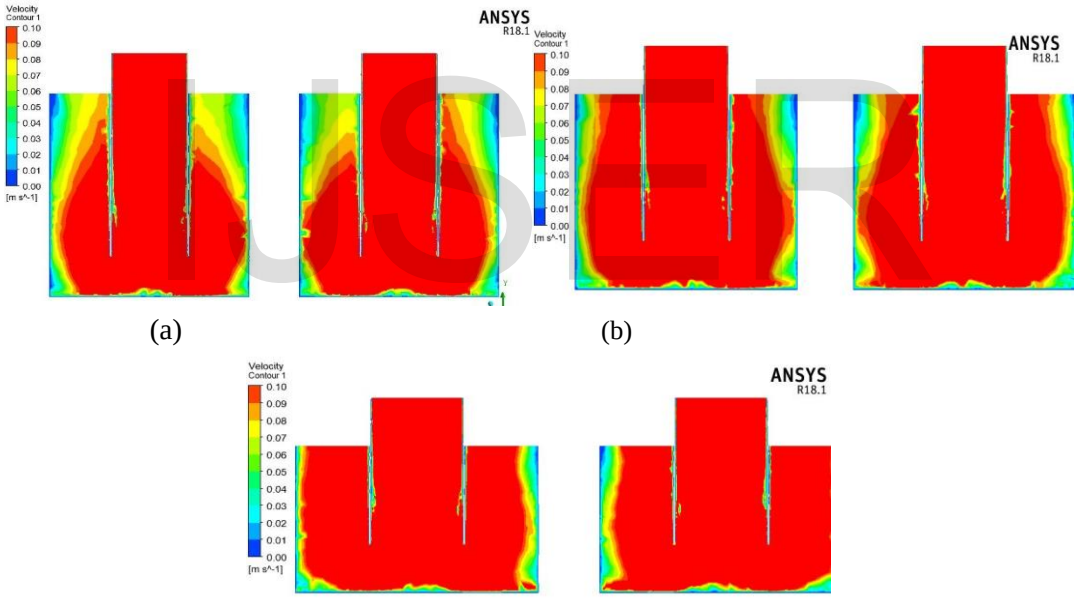

(a) (b)

(c)

Fig. (23) velocity contour along the suction pipe (a) case 7 (b) case8 (c) case9.

Velocity Vectors magnitude at the bottom level of the sump (0m) show in Figure (24). There are separation zones and the dead zone appears and there is an irregularity in velocity vectors as well as the vortices clearly when the sump height increase.

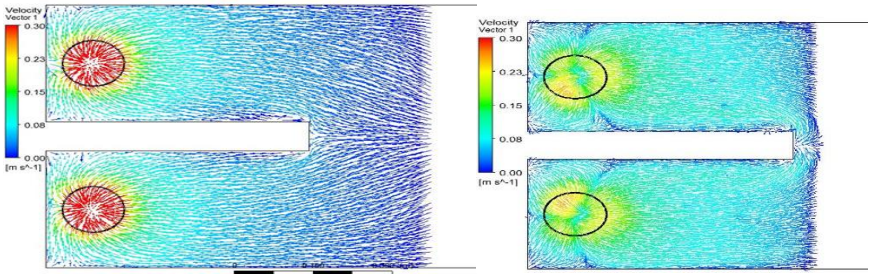

(a) (b)

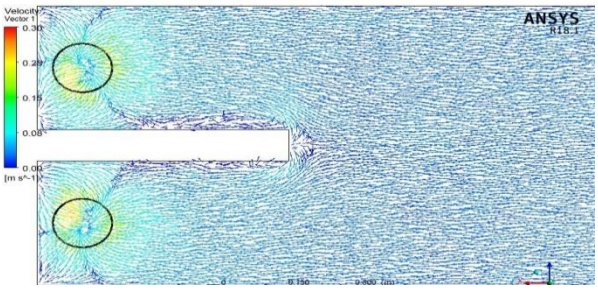

(c)

Fig. (24) velocity vectors at the bottom (0 m) (a) case 1 (b) case8 (c) case9.

The velocity contour at the upper level of water (0.3 m) shown in Figure (25) indicates that the velocity of flow increase when the height of the sump decreases, and there is no dead zone.

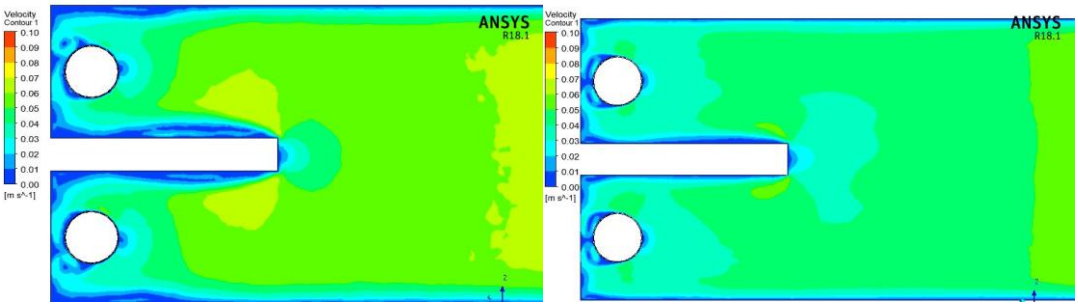

(a) (b)

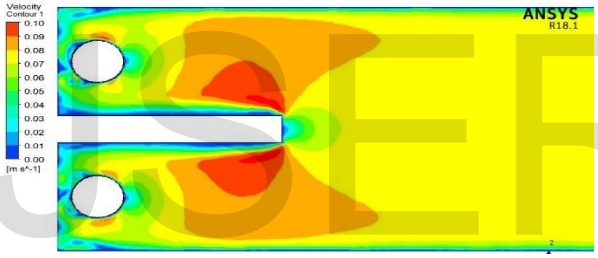

(c)

Fig. (25) velocity contour at the upper level of water (0.3 m) (a) case 7 (b) case8 (c) case9.

Velocity Vectors magnitude at the slop of the canal shown in Figure (26). There are separation zones and the dead zone appears and there is an irregularity in velocity vectors as well as the vortices clearly when the sump height increase.

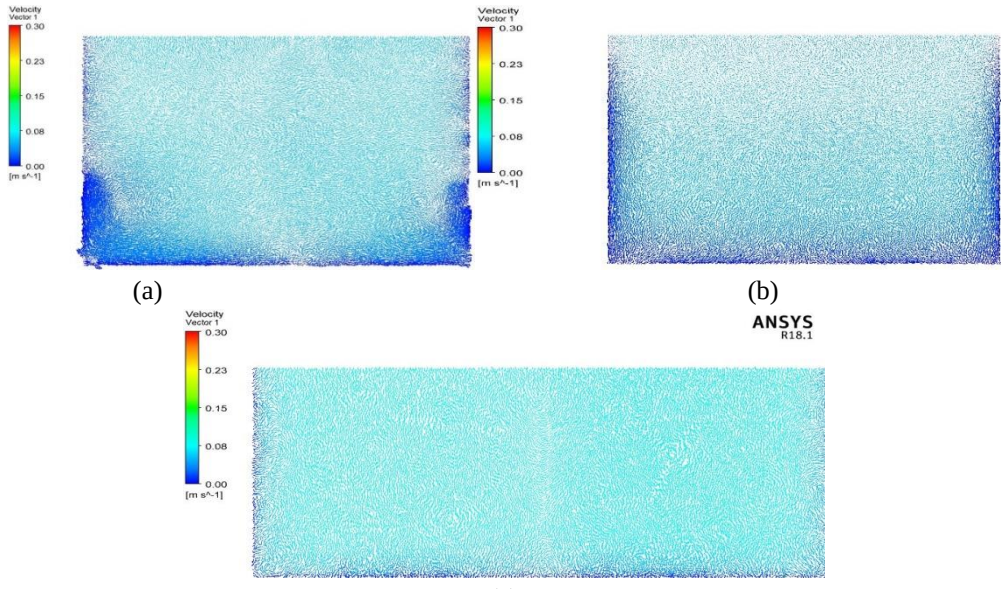

(a) (b)

(c)

Fig. (26) velocity vectors at the slop of canal (a) case 1 (b) case8 (c) case9.

7.4. Swirl Angle Measurements

The swirl angle measurement results will be discussed in this section. There were nine cases conducted in this study, similar to the previous sections. Each of these cases was observed at different water levels and different flow rates. Table (1) show the results of swirl angle of the study. For cases 1,2 and 3 it was observed that a swirl angle of 4.6°, 3.3°, 2.4° respectively. The results indicated that these are not as critical as explained in Table (1). Furthermore, for cases 4, 5, and 6 the flow rates constant at 30L/S with different water level remained. The swirl angles of 9.1°, 11.7°, and 14.2 respectively.

Table (1) Result of swirl and swirl angle of the study

Case of study	Water level (m)	Flow rate, Q (L/s)	Swirl angle (°)
1	0.3	30	4.6
2	0.3	15	3.3
3	0.3	10	2.4
4	0.18	30	9.1
5	0.122	30	11.7
6	0.062	30	14.2
7	0.3	30	4.6
8	0.24	30	7.4
9	0.18	30	9.1

Another group of cases was observed at a maximum flow rate of 30L/s. It was observed that for case 9, the maximum swirl angle was 9.1˚.

For the case 8 and 9, the observed swirl and swirl angles were 54 rev/min and 20 rev/min at 11.7° and 4.4° respectively. From the literature, the adequate typical design required the swirl angle (θ) to be less than 5° [12]. For this situation, cases 1, 2, 3, 6, and 9 produced acceptable values; however, for cases of 4, 5, 7, and 8 observed values did not pass the acceptable value see table (1). The swirl and swirl angle also depend on the water level and flow rate. At the lowest water level (0.18m) with the highest flow rate of 30L/s, the number of swirls and swirl angle was highest noted as 66rev/min and 14.2°. Compared to case 1, at the highest water level, 0.3m and lowest flow rate 10L/s the number of swirls and swirl angles is the smallest, in the range of acceptable value.

9. CONCLUSION

In the computational study, the grid sensitivities and flow visualization have been carried out. The number of the grid element in the model gives effect to the number of iteration process and time to converge. The model that consists of a finer grid has a big number of iteration and took a long time to converge. In the velocity contour visualization, the suction intake (near the entrance of the intake column) has the highest velocity mainly occurred. Different approaches were simulated using CFD to find the optimum and reliable modification method for the pumping station. The CFD analysis yields a complete three-dimensional picture of the velocity contours inside the sump intake. Established as a simulation model, it is proven to be very effective in predicting velocity magnitude (m/s).

In all cases with a water level of 0.3m, even with maximum flow rate (30L/s); there is no occurrence of a vortex during the testing. In other cases, when the water level is low (0.18m) and the maximum flow rate (30L/s), the characteristics of the water flow inside the sump intake show the occurrences of vortices either surface and subsurface. As the water level at the pump sump decreases more vortices spreading in the flow and this allows air entering the suction pipe. As a result, the compressibility of flow and its density decreases and this needs more power for compressing. the increasing discharge in the canal leads to increase water velocity and there is no dead zone in the sump pump in the same section when the water level is constant and The increasing water level in the pump sump leads to increase water velocity and there is no dead zone in the same section when discharge is constant.

Calculations made indicated that the swirl angles of cases 4, 5, 6,8, and 9 were more than 5°. However, it has been confirmed by previous researcher results, that these are not acceptable values. Case 6 is the worst condition of water flow characteristics in this study. In this case, the occurrence of vortices is caused by submergence (minimum water level of 0.062m) and flow rate (maximum flow rate of 30L/s).

REFERENCES

[1] TANWEER S. DESMUKH AND GAHLOT "SIMULATION OF FLOW THROUGH A PUMP SUMP AND ITS VALIDATION", IJRRAS 4 (1), PP.7-17, JULY (2010).

[2] Ashraf Ghanem and Elzahry Farouk Elzahry "Flow Characteristics and Efficiency of Faraskour Pump Sump using Computational Fluid Dynamics (CFD)", APPLICATIONS OF MODELLING AND SIMULATION eISSN 2600-8084 VOL 5, 2021, 7-15.

[3] Cecilia Lucino and Gonzalo Duró, "Vortex Detection in Pump Sumps by Means of CFD", XXIV, Latin American Congress on Hydraulics Punta a Del Este, Uruguay, (IAHR), Nov., (2010).

[4] Franci Rok, Aljaz Skerl and Andrej Lipej, " A Hydraulic Study of Cooling Water Intake Structure" 3rd IAHR International Meeting of the Workgroup on Cavitations and Dynamic Problems in Hydraulic Machinery and Systems, Brno, Czech Republic, Oct. 14-16 (2009).

[5] Elzahry Farouk Elzahry and Ashraf Ghanem "Optimum Design of Pump Intake using CFD for Improving Hydraulic Performance", APPLICATIONS OF MODELLING AND SIMULATION eISSN 2600-8084 VOL 4, 2020, 57-63.

[6] Tsou, John L., B. W. Melville, R. Ettema, and T. Nakato. Review of flow problems at water intake pump sumps. No. CONF-941007-. American Society of Mechanical Engineers, New York, NY (United States), 1994.

[7] Norizan, Tajul A., Eslam Reda, and Zambri Harun. "Enhancement of vorticity reduction by floor splitter in pump sump to improve pump efficiency." Sustainable Energy Technologies and Assessments 26 (2018): 28-36.

[8] Hydraulic Institute. American National Standard for Rotodynamic Pumps for Pump Intake Design. American National Standards Institute, Inc, 2012.

[9] The National Standards Authority of Ireland (NSAI). Rotodynamic Pumps - Design of Pump Intakes Recommendations for Installation of Pumps. Comite Europeen de Normalisation, Brussels, 2009.

[10] TSJ S002: Standard Method for Model Testing the Performance of a Pump Sump, Turbomachinery Society of Japan, Tokyo, 2005.

[11] Tullis, James Paul. "Modeling in design of pumping pits." Journal of the Hydraulics Division 105, no. 9 (1979): 1053-1063.

[12] B. R., James, "Water Pumps and Pumping Systems" McGraw-Hill, New York, (2002).